EUROPEAN ORGANIZATION FOR NUCLEAR RESEARCH (CERN)

CERN-EP-2021-108
LHCb-PAPER-2021-013
19 July 2022



# Study of coherent $J/\psi$ production in lead-lead collisions at $\sqrt{s_{\rm NN}} = 5\,\text{TeV}$

LHCb collaboration[†]

**Abstract**

Coherent production of $J/\psi$ mesons is studied in ultraperipheral lead-lead collisions at a nucleon-nucleon centre-of-mass energy of 5 TeV, using a data sample collected by the LHCb experiment corresponding to an integrated luminosity of about $10\,\mu\text{b}^{-1}$. The $J/\psi$ mesons are reconstructed in the dimuon final state and are required to have transverse momentum below 1 GeV. The cross-section within the rapidity range of $2.0 < y < 4.5$ is measured to be $4.45 \pm 0.24 \pm 0.18 \pm 0.58\,\text{mb}$, where the first uncertainty is statistical, the second systematic and the third originates from the luminosity determination. The cross-section is also measured in $J/\psi$ rapidity intervals. The results are compared to predictions from phenomenological models.

Published in JHEP 07 (2022) 117



[†]Authors are listed at the end of this paper.

# 1 Introduction

In ultra-relativistic collisions of heavy-nuclei at the LHC, vector mesons can be produced through two-photon and photonuclear interactions in ultraperipheral collisions (UPCs), where the two nuclei collide with an impact parameter larger than the sum of their radii. The cross-sections for photon-induced reactions are large because the intensity of the photon flux is enhanced by the strong electromagnetic field of the nucleus, which increases with the square of the atomic number. The interactions are either coherent, where the photon couples to all nucleons, or incoherent, where the photon couples to a single nucleon. In the incoherent case the nucleus is likely to break up, leading to a higher transverse momentum, $p_{\rm T}$, of the meson. Coherent $J/\psi$-meson production in UPCs can be described by the interaction of photons with gluons identified as a single object with vacuum quantum numbers. This is commonly modelled as a pomeron ($\mathbb{P}$) exchange [1–5].

An illustration of this process is given in Fig. 1. This interaction probes the gluon distribution at a hard momentum transfer $Q^2$ of about $m^2_{J/\psi}/4$, where $m_{J/\psi}$ is the $J/\psi$ mass [6, 7].[1] In this paper, a measurement of coherent $J/\psi$ production is reported in lead-lead collisions at a nucleon-nucleon centre-of-mass energy of $\sqrt{s_{\rm NN}} = 5\,\text{TeV}$ collected with the LHCb detector in 2015, corresponding to an integrated luminosity of about $10\,\mu\text{b}^{-1}$. The forward rapidity range $2.0 < y < 4.5$ covered by the present measurement corresponds to values of the Bjorken variable $x \approx (m_{J/\psi}/\sqrt{s_{\rm NN}})e^{\pm y}$ down to $10^{-5}$. At these $x$ values, current uncertainties on the gluon distributions inside the nucleon are sizeable [8, 9], thus new measurements should reduce the uncertainties [10–12]. Results of UPC studies have also been reported by RHIC and LHC experiments [13–23]. In particular, recent measurements in the forward rapidity region $2.5 < y < 4.0$ [20] by the ALICE Collaboration show the importance of including nuclear modification effects in theoretical models.

The paper is organised as follows. The LHCb detector and the event selection are

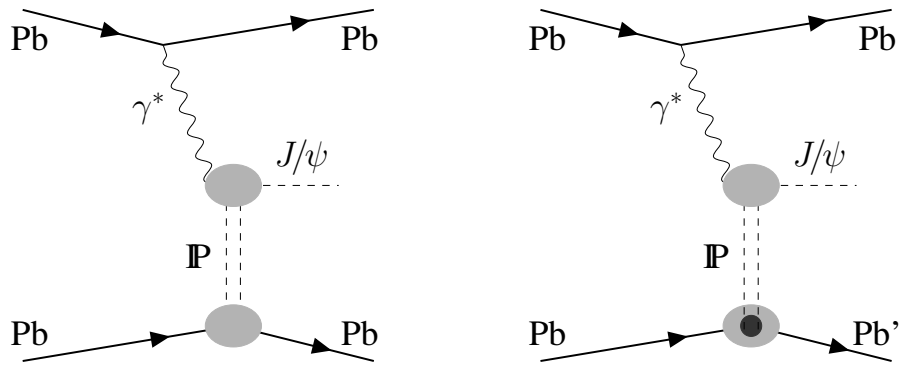


Figure 1: Illustration of the (left) coherent scatter with the lead nucleus and (right) incoherent interaction with a single nucleon leading to exclusive production of $J/\psi$ mesons in ultraperipheral heavy-ion collisions. The symbol Pb' represents any final state for the nucleus inelastic scattering in the incoherent process.

[1] In this paper natural units where $c = 1$ are used.

described in Sec. 2. The analysis strategy and the systematic uncertainties are discussed in Secs. 3 and 4, respectively. The differential cross-section results for $J/\psi$ production in UPCs are detailed in Sec. 5. Conclusions are given in Sec. 6.

# 2 Detector description and candidate selection

The LHCb detector [24, 25] is a single-arm forward spectrometer covering the pseudorapidity range $2 < \eta < 5$, designed for the study of particles containing $b$ or $c$ quarks. The detector includes a high-precision tracking system consisting of a silicon-strip vertex detector (VELO) surrounding the interaction region, a silicon-strip detector located upstream of a dipole magnet with a bending power of about 4 Tm, and three stations of silicon-strip detectors and straw drift tubes placed downstream of the magnet. The tracking system provides a measurement of momentum, $p$, of charged particles with a relative uncertainty that varies from 0.5% at low momentum to 1.0% at 200 GeV. The VELO has a material budget of one fifth of a radiation length that allows reconstruction and rejection of events with additional low-momentum tracks [26]. Different types of charged hadrons are distinguished using information from two ring-imaging Cherenkov detectors. Photons, electrons and hadrons are identified by a calorimeter system consisting of scintillating-pad (SPD) and preshower (PRS) detectors, an electromagnetic calorimeter and a hadronic calorimeter. Muons are identified by a system composed of alternating layers of iron and multiwire proportional chambers. The pseudorapidity coverage is extended by forward shower counters (HeRSCheL) consisting of five planes of scintillators with three planes at 114, 19.7 and 7.5 m upstream of the interaction point, and two downstream at 20 and 114 m. The HeRSCheL detector significantly extends the acceptance in which hadron showers can be detected to classify central exclusive production and UPC events by covering a pseudorapidity region of approximately $-10 < \eta < -5$ and $5 < \eta < 10$ [27]. The real-time event selection is performed by a trigger, which consists of a hardware stage, based on information from the calorimeter and muon systems, followed by a software stage, which applies a full event reconstruction.

In this analysis, $J/\psi$ candidates are selected through their decays into two oppositely charged muons. The events are selected by the trigger system, requiring information from the muon system to be compatible with at least one muon with $p_{\mathrm{T}}$ larger than 900 MeV at the hardware level, and the invariant mass of the two muons, $m_{\mu^+\mu^-}$, exceeding 2.7 GeV at the software level. In the offline selection, candidates are identified by requiring both muons to have $p_{\mathrm{T}} > 800$ MeV within the pseudorapidity region $2.0 < \eta < 4.5$, and $m_{\mu^+\mu^-}$ to be within 65 MeV of the known $J/\psi$ mass [28]. Only $J/\psi$ candidates with reconstructed $p_{\mathrm{T}} < 1$ GeV and an azimuthal opening angle between the muons larger than $0.9\pi$ are retained.

In order to suppress background from more central lead-lead collisions, events with more than 20 deposits in the SPD are vetoed. In addition, events with an extra VELO track in the spatial vicinity of the reconstructed $J/\psi$ candidate are rejected. Finally, a requirement on the activity in the HeRSCheL detector, based upon a figure-of-merit that combines detector signals of all stations [27], is used to discard events with significant activity in the HeRSCheL acceptance region.

# 3 Cross-section measurement

The differential cross-section for coherent $J/\psi$ production is evaluated as

$$\frac{d\sigma}{dy} = \frac{n_{\rm coh}}{\varepsilon_y \, \Delta y \, \mathcal{L} \, \mathcal{B}} \,, \tag{1}$$

where $n_{\rm coh}$ is the signal yield, $\varepsilon_y$ is the total efficiency in each rapidity interval, $\Delta y$ is the rapidity interval width, $\mathcal{L}$ is the integrated luminosity, and $\mathcal{B} = (5.961 \pm 0.033)\%$ is the $J/\psi \to \mu^+\mu^-$ branching fraction [28].

The luminosity is determined with the same method as for proton-proton collisions [29, 30]. Interaction rates are determined from random luminosity triggers and are encapsulated in a small number of luminosity sensitive observables. These observables include the number of vertices and tracks in the VELO, the number of identified muons, the number of hits in the SPD, and the transverse energy deposition in the calorimeters. Whereas the rates from the different observables are consistent in proton-proton and proton-lead collisions, in lead-lead collisions some discrepancies are observed, which are used to assign a systematic uncertainty. The integrated luminosity of the data sample is determined to be $10.1 \pm 1.3\,\mu{\rm b}^{-1}$, where the absolute calibration is performed with Van der Meer scans [30]. The luminosity determination is checked using the ratio of $\gamma\gamma \to \mu^+\mu^-$ events over coherent $J/\psi$ events in the range of the measurement. This ratio was found within 10% of the ratio predicted by SuperChic 4 [31] using the `MMHT2015qed NNLO` probability density function setting [32] for both the differential and the integrated cross-section ratio.

## 3.1 Signal yield determination

The signal yield is determined in two steps. First, a fit to the dimuon invariant mass spectrum is performed to obtain the $J/\psi$ yield, which includes the contribution of coherent and incoherent $J/\psi$ mesons, and feed-down from $J/\psi$ mesons originating from $\psi(2S)$ decays. Second, a fit to the $J/\psi$ transverse momentum is used to isolate the coherent $J/\psi$ yield.

The yield of $J/\psi$ mesons is estimated by fitting the dimuon invariant mass distribution to signal and background components. The $J/\psi$ and $\psi(2S)$ mass shapes are modelled by double-sided Crystal Ball functions [33], and the nonresonant background by an exponential function multiplied by a first-order polynomial function. The $\psi(2S)$ parameters, aside from the mean, are constrained to be the same as for the $J/\psi$ meson. The fit is performed in the range $2.7 < m_{\mu^+\mu^-} < 4\,{\rm GeV}$. The dimuon mass distribution along with the fit projection is shown in Fig. 2.

For the determination of the coherent yield two resonant background sources are considered: incoherent $J/\psi$ photoproduction and $J/\psi$ meson feed-down from photoproduced $\psi(2S)$ decays. In order to determine the signal yield in the presence of these backgrounds, an unbinned maximum-likelihood fit to the natural logarithm of the transverse momentum squared, $\log(p_{\rm T}^2)$, of $J/\psi$ candidates inside the chosen mass window is performed. The signal and background probability density functions are estimated using the StarLight generator [2] and the LHCb detector simulation. The amount of nonresonant background is constrained by the dimuon invariant mass fit. The feed-down background is assumed to have the same $\log(p_{\rm T}^2)$ distribution as simulated $\psi(2S) \to J/\psi\,\pi^+\pi^-$ decays, where the $J/\psi$

Table 1: Total and coherent $J/\psi$ yields after the invariant mass and the transverse momentum fits, in $J/\psi$ rapidity intervals.

| Rapidity $y$ | Total $J/\psi$ yield | Coherent $J/\psi$ yield |
|---|---|---|
| $2.0-2.5$ | $69 \pm 9$ | $53 \pm 8$ |
| $2.5-3.0$ | $208 \pm 15$ | $153 \pm 14$ |
| $3.0-3.5$ | $233 \pm 16$ | $176 \pm 15$ |
| $3.5-4.0$ | $131 \pm 12$ | $95 \pm 11$ |
| $4.0-4.5$ | $32 \pm 6$ | $12 \pm 5$ |

is reconstructed and both pions escape the rejection requirements on additional tracks. Figure 3 shows the $\log(p_{\rm T}^2)$ data distribution along with the fit projection in the rapidity interval $2.5 < y < 3$. All $J/\psi$ yields are reported in Table 1.

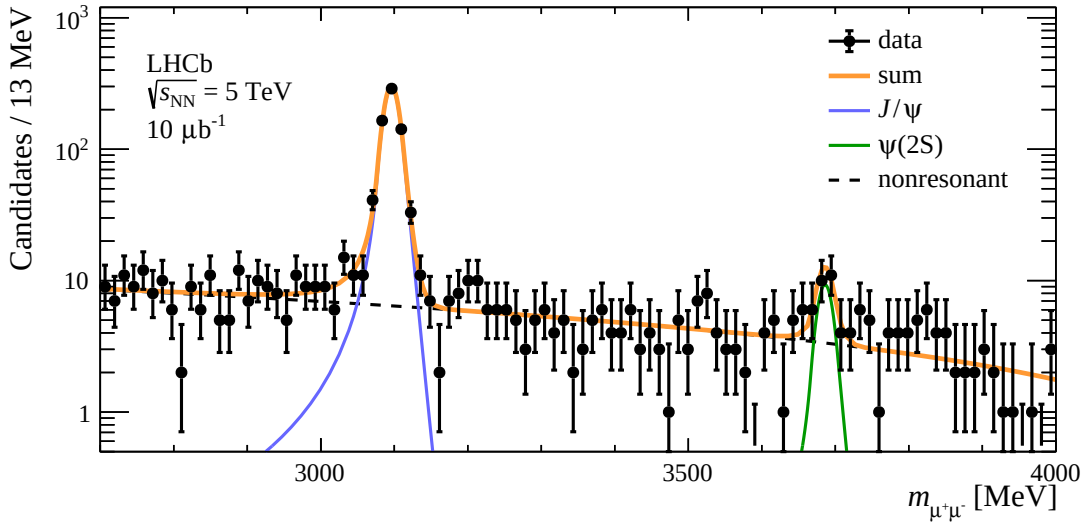


Figure 2: The dimuon invariant mass spectrum in the range between 2.7 and 4.0 GeV. The contribution of $J/\psi$ (solid purple line) and $\psi(2S)$ (solid dark green line) mesons, and non-resonant background (dashed black line) are shown individually along with the sum of all contributions (solid orange line).

## 3.2 Efficiency determination

For any given $J/\psi$ rapidity interval, the total efficiency is evaluated as the product of the acceptance and the reconstruction and selection efficiencies. The acceptance includes the requirements on the kinematic properties of the $J/\psi$ decay products, and is evaluated using a sample of coherently photoproduced $J/\psi \to \mu^+\mu^-$ events produced with the STARlight event generator. In this paper the charmonium polarisation is assumed to be the same as that of the photon and thus fully transverse as it is implemented in the STARlight event generator. The reconstruction efficiency includes track reconstruction and muon identification. The selection efficiency includes requirements on the SPD deposits,

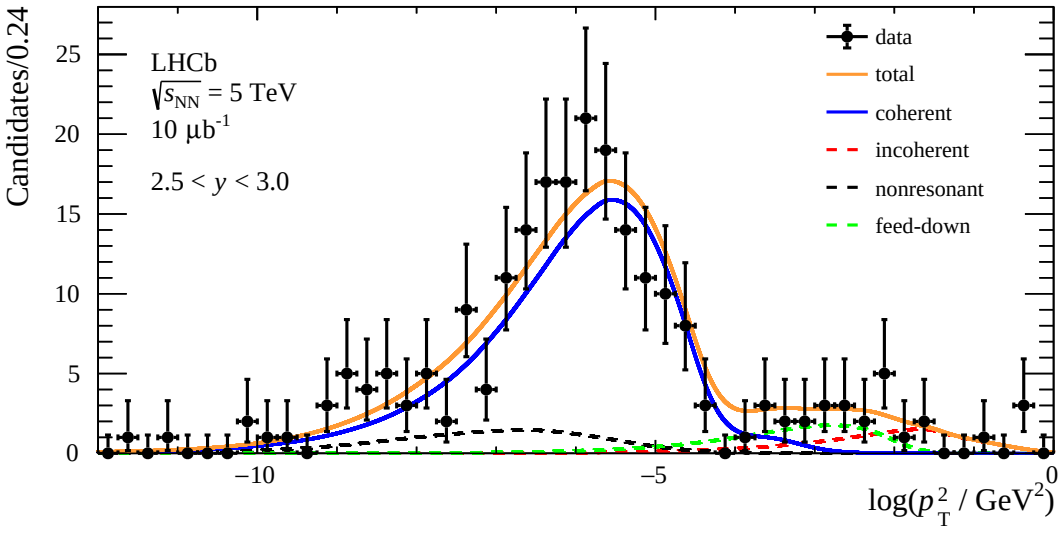


Figure 3: The $\log(p_{\mathrm{T}}^2)$ distribution of dimuon candidates in the interval $2.5 < y < 3.0$, with $p_{\mathrm{T}}$ given in GeV, after all requirements have been applied. The solid orange line represents the combined fit to data; the solid blue line shows the coherent contribution; the incoherent component is displayed by the dashed red line; and the dashed green (black) line shows the feed-down (nonresonant) components.

VELO track multiplicities, and dimuon invariant mass. The hardware trigger efficiency is determined using simulated events, calibrated with data. The software trigger efficiency is measured using $J/\psi$ candidates in events selected with a minimum bias trigger requiring at least one VELO track. Partially reconstructed inclusive $J/\psi \to \mu^+\mu^-$ candidates from proton-proton collision data at a centre-of-mass energy $\sqrt{s}$=13 TeV are used to evaluate the tracking efficiency [34]. The muon identification efficiency has been determined from simulated events generated with the STARLIGHT generator in lead-lead collisions and validated with lead-lead data.

The dimuon invariant mass requirement efficiency is determined using the integral of the double-sided Crystal Ball function. A similar method is used to determine the efficiencies of the multiplicity requirements on the VELO tracks and SPD deposits. The veto efficiency of the HeRSCheL detector activity is evaluated with a sample of nonresonant dimuon events from lead-lead data using a fit obtained from STARLIGHT simulated $\gamma\gamma \to \mu^+\mu^-$ events, and comparing the number of events satisfying and failing the requirement. The total efficiency for this selection is about 90%.

# 4 Systematic uncertainties

Systematic uncertainties on the measured cross-section are considered from the integrated luminosity calculation, the determination of the muon reconstruction and selection efficiencies, the trigger efficiency, the mass fit signal model, the modelling of the feed-down background, and the knowledge of the $J/\psi \to \mu^+\mu^-$ branching fraction. They are described below and summarised in Table 2. The largest uncertainty originates from the integrated luminosity determination and is estimated to be 13%.

The uncertainties related to the $J/\psi$ reconstruction efficiency include effects on the

track reconstruction and muon identification, and they are dominated by the limited size of the control sample. Several contributions to the selection efficiency are considered. The impact of the requirement on the SPD multiplicity is estimated from a data control sample. Effects related to the dimuon invariant mass efficiency are taken from the uncertainty of the integral of the double-sided Crystal Ball function. The inefficiency of the VELO track multiplicity requirement is found to be negligible and no uncertainty is assigned. The uncertainty due to the HeRSCheL selection is estimated by comparing the efficiency evaluated in different samples, selected by applying requirements that do not affect the signal.

The efficiency of the hardware trigger is determined from simulated events. It is compared to the efficiency obtained on a smaller data sample selected by independent triggers, and the difference is taken as systematic uncertainty. The software-stage trigger efficiency evaluation is cross-checked with an independent estimation based on data, where events are selected with a different trigger requirement. The efficiencies are consistent within statistical uncertainties, which are used to assign a systematic uncertainty.

Possible cross-section variations associated to the signal model in the fit to the dimuon invariant mass spectrum is assessed using an alternative model. A Bukin function [35] is used for the signal and the difference in the signal yields with respect to the default fit is assigned as uncertainty.

In order to estimate the systematic uncertainty due to the feed-down component, the $J/\psi$ candidate selection is modified to select a mixture of coherently and incoherently produced $\psi(2S) \to J/\psi\,\pi^+\pi^-$ events. After requiring the reconstructed mass of the $\psi(2S)$ candidates to be within 65 MeV of the known $\psi(2S)$ mass [28], 22 candidates are obtained. In the simulation, $\psi(2S) \to J/\psi\,\pi^+\pi^-$ events are used as a proxy for all $\psi(2S) \to J/\psi\,X$ feed-down. The ratio between $\psi(2S) \to J/\psi\,\pi^+\pi^-$ candidates, where the pions left no VELO track, and fully reconstructed candidates is determined and scaled assuming that $\psi(2S) \to J/\psi\,\pi^+\pi^-$ events are representative for all $\psi(2S) \to J/\psi\,X$ events. From this ratio and the $J/\psi$ yield, the number of $J/\psi \to \mu^+\mu^-$ candidates originating from $\psi(2S)$ decays in the signal sample is determined to be $42.5 \pm 9.1$. This yield is assigned to the different intervals in meson rapidity using a template from simulated coherent $\psi(2S) \to J/\psi\,\pi^+\pi^-$ events. The uncertainty is dominated by the limited size of the data sample.

# 5 Results and discussion

Using Eq. (1), the cross-section for coherent $J/\psi$ production within the fiducial region is determined to be

$$\sigma = 4.45 \pm 0.24 \pm 0.18 \pm 0.58\,\text{mb},$$

where the first uncertainty is statistical, the second is systematic and the third is due to the luminosity determination. The $J/\psi$ candidates are reconstructed from dimuon final states, where the muons are detected within the pseudorapidity region $2.0 < \eta < 4.5$ and the $J/\psi$ meson is required to have $p_{\rm T} < 1\,\text{GeV}$ and $2.0 < y < 4.5$. The coherent $J/\psi$ production cross-section, measured in $J/\psi$ rapidity intervals, is given in Table 3. A comparison of the measured differential cross-section with the theoretical predictions discussed below is shown in Fig. 4.

In the model of Gonçalves et al. [4, 36], the cross-section is calculated within the framework of the Colour-Dipole model. Three different parametrisations of the dipole-

Table 2: Systematic uncertainties considered for the differential cross-section measurement of coherent $J/\psi$ production, relative to the central value. Uncertainty ranges correspond to variation over the rapidity intervals. The dominant uncertainty arises from the luminosity determination and is correlated over all intervals.

| Source | Relative uncertainty (%) |
|---|---|
| Luminosity | 13.0 |
| $J/\psi$ reconstruction efficiency | 1.7–4.8 |
| Selection efficiency | 1.7 |
| HeRSCheL requirement efficiency | 1.0 |
| Hardware trigger efficiency | 1.0 |
| Software trigger efficiency | 1.0 |
| Mass fit model | $1.0 - 1.6$ |
| Feed-down background | $0.4 - 1.0$ |
| $J/\psi$ branching fraction | 0.6 |

proton cross-section (IIM, IP-SAT, bCGC), including saturation effects at low Bjorken-x, are combined with two different models of vector-meson wave functions, namely boosted Gaussian (BG) and Gauss-LC (GLC). All the parameters are tuned using HERA data [37–39]. The solid (dashed) curves in Fig. 4 correspond to the IP-SAT+GLC (IIM+BG) model. The combination of IIM [40] with the boosted Gaussian wave function is disfavoured by the data.

The model from Cepila et al. [41] is a variation of the Colour-Dipole model. The main differences with respect to Gonçalves et al. come from the parametrisation of the dipole-proton cross-section and the prescription used to propagate it to the dipole-nucleus scattering amplitudes. In this model, the Glauber-Gribov methodology (GG) or a geometric scaling between the nuclear saturation scale and the saturation scale in the proton (GS) are used. Both prescriptions are able to describe the data.

In the model proposed by Mäntysaari et al. [42], the cross-section is also calculated using the Colour-Dipole model including subnucleon scale fluctuations. Predictions with and without subnucleonic fluctuations using the IP-SAT parametrisation for the dipole-proton cross-section and the GLC for the vector-meson wave function are compared to this measurement. Both prescriptions are able to describe the data.

The model provided by Guzey et al. [1] is based on a perturbative QCD calculation. The coherent $J/\psi$ production cross-section on a proton target is calculated at leading order within the leading-log approximation. Different models for the nuclear structure are used: weaker (LTA_W) and stronger (LTA_S) nuclear shadowing scenarios with a leading twist nuclear shadowing model [43] as well as EPS09 [8] nuclear parton distribution functions. The measurement can be described by these models.

The coherent photoproduction cross-section of $J/\psi$ mesons in the forward region measured by the ALICE collaboration [20] uses an integrated luminosity ten times larger in a smaller region of rapidity compared to this measurement. In the kinematic region were the two experiments overlap the ALICE cross-section is reported about 35% larger, with approximately a 30% smaller uncertainty, leading to a discrepancy at the level of 2.3 standard deviations.

Table 3: Measured cross-section $\sigma$ with breakdown of statistical, systematic and luminosity uncertainties measured as a function of the $J/\psi$ rapidity. Note that the cross-sections are not normalised by the $y$ interval width.

| $y$ interval | $\sigma$ [mb] | Stat. [mb] | Syst. [mb] | Lumi. [mb] |
|---|---|---|---|---|
| $2.0-4.5$ | 4.45 | 0.24 | 0.18 | 0.58 |
| $2.0-2.5$ | 1.35 | 0.19 | 0.06 | 0.17 |
| $2.5-3.0$ | 1.09 | 0.09 | 0.05 | 0.14 |
| $3.0-3.5$ | 0.89 | 0.07 | 0.04 | 0.12 |
| $3.5-4.0$ | 0.65 | 0.06 | 0.03 | 0.08 |
| $4.0-4.5$ | 0.48 | 0.09 | 0.02 | 0.06 |

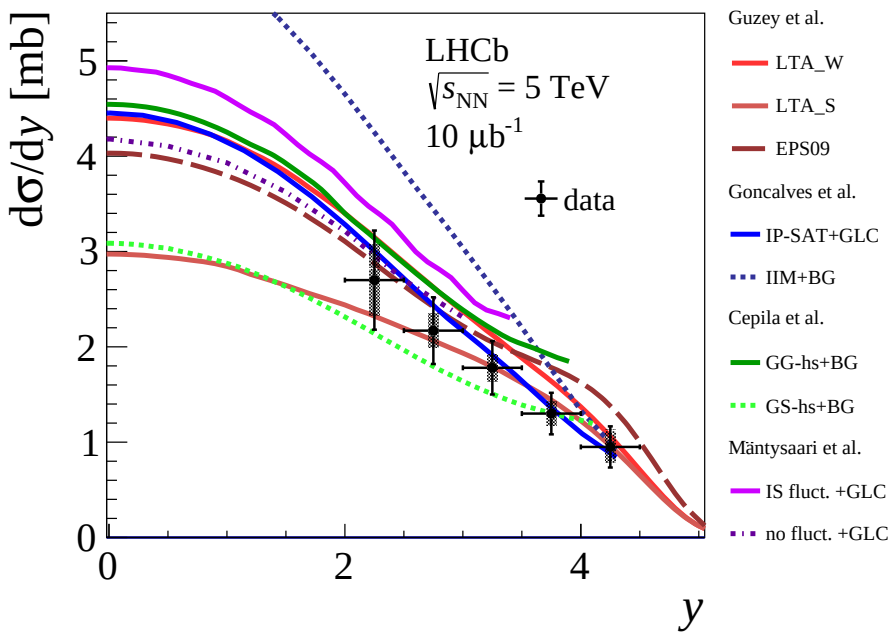


Figure 4: Differential cross-section as a function of rapidity for coherent $J/\psi$ production compared to different phenomenological predictions [1,4,36,41,42]. The measurements are shown as points, where inner and outer error bars represent the statistical and the total uncertainties, respectively. This includes the uncertainty on the luminosity and is therefore highly correlated.

# 6 Conclusions

The coherent $J/\psi$ production cross-section in lead-lead collisions at $\sqrt{s_{\rm NN}} = 5\,\text{TeV}$, using a data sample collected by the LHCb experiment and corresponding to an integrated luminosity of about $10\,\mu\text{b}^{-1}$, is measured to be $4.45 \pm 0.24 \pm 0.18 \pm 0.58\,\text{mb}$, where the first uncertainty is statistical, the second is systematic and the third is due to the luminosity determination. The measurement uses $J/\psi$ mesons reconstructed in the dimuon final state with $p_{\rm T} < 1\,\text{GeV}$ and $2.0 < y < 4.5$, where muons are detected within the pseudorapidity region $2.0 < \eta < 4.5$. The cross-section is also measured in five $J/\psi$ rapidity intervals and

the results are compared to predictions from different phenomenological models. Future measurements with different mesons and larger data samples will further constrain these models.

# Acknowledgements

We express our gratitude to our colleagues in the CERN accelerator departments for the excellent performance of the LHC. We thank the technical and administrative staff at the LHCb institutes. We acknowledge support from CERN and from the national agencies: CAPES, CNPq, FAPERJ and FINEP (Brazil); MOST and NSFC (China); CNRS/IN2P3 (France); BMBF, DFG and MPG (Germany); INFN (Italy); NWO (Netherlands); MNiSW and NCN (Poland); MEN/IFA (Romania); MSHE (Russia); MICINN (Spain); SNSF and SER (Switzerland); NASU (Ukraine); STFC (United Kingdom); DOE NP and NSF (USA). We acknowledge the computing resources that are provided by CERN, IN2P3 (France), KIT and DESY (Germany), INFN (Italy), SURF (Netherlands), PIC (Spain), GridPP (United Kingdom), RRCKI and Yandex LLC (Russia), CSCS (Switzerland), IFIN-HH (Romania), CBPF (Brazil), PL-GRID (Poland) and NERSC (USA). We are indebted to the communities behind the multiple open-source software packages on which we depend. Individual groups or members have received support from ARC and ARDC (Australia); AvH Foundation (Germany); EPLANET, Marie Skłodowska-Curie Actions and ERC (European Union); A*MIDEX, ANR, Labex P2IO and OCEVU, and Région Auvergne-Rhône-Alpes (France); Key Research Program of Frontier Sciences of CAS, CAS PIFI, CAS CCEPP, Fundamental Research Funds for the Central Universities, and Sci. & Tech. Program of Guangzhou (China); RFBR, RSF and Yandex LLC (Russia); GVA, XuntaGal and GENCAT (Spain); the Leverhulme Trust, the Royal Society and UKRI (United Kingdom).

# References

[1] V. Guzey, E. Kryshen, and M. Zhalov, *Coherent photoproduction of vector mesons in ultraperipheral heavy ion collisions: Update for run 2 at the CERN Large Hadron Collider*, Phys. Rev. **C93** (2016) 055206, arXiv:1602.01456.

[2] S. R. Klein *et al.*, *STARlight: A Monte Carlo simulation program for ultra-peripheral collisions of relativistic ions*, Comput. Phys. Commun. **212** (2017) 258, arXiv:1607.03838.

[3] A. Adeluyi and C. A. Bertulani, *Constraining gluon shadowing using photoproduction in ultraperipheral pA and AA collisions*, Phys. Rev. **C85** (2012) 044904, arXiv:1201.0146.

[4] V. P. Gonçalves and M. V. T. Machado, *Vector meson production in coherent hadronic interactions: an update on predictions for RHIC and LHC*, Phys. Rev. **C84** (2011) 011902, arXiv:1106.3036.

[5] A. Cisek, W. Schäfer, and A. Szczurek, *Exclusive coherent production of heavy vector mesons in nucleus-nucleus collisions at LHC*, Phys. Rev. **C86** (2012) 014905, arXiv:1204.5381.

[6] C. A. Bertulani, S. R. Klein, and J. Nystrand, *Physics of ultra-peripheral nuclear collisions*, Ann. Rev. Nucl. Part. Sci. **55** (2005) 271, arXiv:nucl-ex/0502005.

[7] M. G. Ryskin, *Diffractive J/$\psi$ electroproduction in LLA QCD*, Z. Phys. **C57** (1993) 89.

[8] K. J. Eskola, H. Paukkunen, and C. A. Salgado, *EPS09: A new generation of NLO and LO nuclear parton distribution functions*, JHEP **04** (2009) 065, arXiv:0902.4154.

[9] K. J. Eskola, P. Paakkinen, H. Paukkunen, and C. A. Salgado, *EPPS16: Nuclear parton distributions with LHC data*, Eur. Phys. J. **C77** (2017) 163, arXiv:1612.05741.

[10] C. A. Flett *et al.*, *Towards a determination of the low x gluon via exclusive J/$\psi$ production*, PoS **DIS2019** (2019) 053, arXiv:1907.06471.

[11] C. A. Flett *et al.*, *How to include exclusive J/$\psi$ production data in global PDF analyses*, Phys. Rev. **D101** (2020) 094011, arXiv:1908.08398.

[12] K. Kovarik *et al.*, *nCTEQ15 - Global analysis of nuclear parton distributions with uncertainties in the CTEQ framework*, Phys. Rev. **D93** (2016) 085037, arXiv:1509.00792.

[13] PHENIX collaboration, S. Afanasiev *et al.*, *Photoproduction of J/$\psi$ and of high mass $e^+e^-$ in ultra-peripheral Au+Au collisions at $\sqrt{s_{\rm NN}} = 200\,$GeV*, Phys. Lett. **B679** (2009) 321, arXiv:0903.2041.

[14] STAR collaboration, J. Adams *et al.*, *Production of $e^+e^-$ pairs accompanied by nuclear dissociation in ultra-peripheral heavy ion collision*, Phys. Rev. **C70** (2004) 031902, arXiv:nucl-ex/0404012.

[15] CMS collaboration, V. Khachatryan *et al.*, *Coherent J/$\psi$ photoproduction in ultra-peripheral PbPb collisions at $\sqrt{s_{\rm NN}} = 2.76$ TeV with the CMS experiment*, Phys. Lett. **B772** (2017) 489, arXiv:1605.06966.

[16] ALICE collaboration, B. Abelev *et al.*, *Coherent J/$\psi$ photoproduction in ultra-peripheral Pb-Pb collisions at $\sqrt{s_{\rm NN}} = 2.76$ TeV*, Phys. Lett. **B718** (2013) 1273, arXiv:1209.3715.

[17] ALICE collaboration, E. Abbas *et al.*, *Charmonium and $e^+e^-$ pair photoproduction at mid-rapidity in ultra-peripheral Pb-Pb collisions at $\sqrt{s_{\rm NN}} = 2.76$ TeV*, Eur. Phys. J. **C73** (2013) 2617, arXiv:1305.1467.

[18] ALICE collaboration, B. B. Abelev *et al.*, *Exclusive J/$\psi$ photoproduction off protons in ultra-peripheral p-Pb collisions at $\sqrt{s_{\rm NN}} = 5.02$ TeV*, Phys. Rev. Lett. **113** (2014) 232504, arXiv:1406.7819.

[19] ALICE collaboration, J. Adam *et al.*, *Coherent $\rho^0$ photoproduction in ultra-peripheral Pb-Pb collisions at $\sqrt{s_{\rm NN}} = 2.76$ TeV*, JHEP **09** (2015) 095, arXiv:1503.09177.

[20] ALICE collaboration, S. Acharya *et al.*, *Coherent J/$\psi$ photoproduction at forward rapidity in ultra-peripheral Pb-Pb collisions at $\sqrt{s_{\rm NN}} = 5.02$ TeV*, Phys. Lett. **B798** (2019) 134926, arXiv:1904.06272.

[21] ALICE collaboration, S. Acharya *et al.*, *First measurement of coherent $\rho^0$ photoproduction in ultra-peripheral Xe–Xe collisions at $\sqrt{s_{\rm NN}}$=5.44 TeV*, Phys. Lett. **B820** (2021) 136481, arXiv:2101.02581.

[22] ALICE collaboration, S. Acharya *et al.*, *Coherent J/$\psi$ and $\psi'$ photoproduction at midrapidity in ultra-peripheral Pb-Pb collisions at $\sqrt{s_{\rm NN}}$ = 5.02 TeV*, arXiv:2101.04577.

[23] ALICE collaboration, S. Acharya *et al.*, *First measurement of the $|t|$-dependence of coherent J/$\psi$ photonuclear production*, Phys. Lett. **B817** (2021) 136280, arXiv:2101.04623.

[24] LHCb collaboration, A. A. Alves Jr. *et al.*, *The LHCb detector at the LHC*, JINST **3** (2008) S08005.

[25] LHCb collaboration, R. Aaij *et al.*, *LHCb detector performance*, Int. J. Mod. Phys. **A30** (2015) 1530022, arXiv:1412.6352.

[26] R. Aaij *et al.*, *Performance of the LHCb Vertex Locator*, JINST **9** (2014) P09007, arXiv:1405.7808.

[27] K. Carvalho Akiba *et al.*, *The HeRSCheL detector: high-rapidity shower counters for LHCb*, JINST **13** (2018) P04017, arXiv:1801.04281.

[28] Particle Data Group, P. A. Zyla *et al.*, *Review of particle physics*, Prog. Theor. Exp. Phys. **2020** (2020) 083C01.

[29] LHCb collaboration, R. Aaij *et al.*, *Absolute luminosity measurements with the LHCb detector at the LHC*, JINST **7** (2012) P01010, arXiv:1110.2866.

[30] LHCb collaboration, R. Aaij *et al.*, *Precision luminosity measurements at LHCb*, JINST **9** (2014) P12005, arXiv:1410.0149.

[31] L. A. Harland-Lang, M. Tasevsky, V. A. Khoze, and M. G. Ryskin, *A new approach to modelling elastic and inelastic photon-initiated production at the LHC: SuperChic 4*, Eur. Phys. J. C **80** (2020) 925, arXiv:2007.12704.

[32] L. A. Harland-Lang, A. D. Martin, R. Nathvani, and R. S. Thorne, *Ad Lucem: QED Parton Distribution Functions in the MMHT Framework*, Eur. Phys. J. C **79** (2019) 811, arXiv:1907.02750.

[33] T. Skwarnicki, *A study of the radiative cascade transitions between the Upsilon-prime and Upsilon resonances*, PhD thesis, Institute of Nuclear Physics, Krakow, 1986, DESY-F31-86-02.

[34] M. Adinolfi *et al.*, *Performance of the LHCb RICH detector at the LHC*, Eur. Phys. J. **C73** (2013) 2431, arXiv:1211.6759.

[35] A. D. Bukin, *Fitting function for asymmetric peaks*, arXiv:0711.4449.

[36] V. P. Gonçalves *et al.*, *Color dipole predictions for the exclusive vector meson photoproduction in pp, pPb, and PbPb collisions at run 2 LHC energies*, Phys. Rev. **D96** (2017) 094027, arXiv:1710.10070.

[37] V. P. Gonçalves and M. V. T. Machado, *Quarkonium production in coherent hadron-hadron interactions at the LHC*, Phys. Rev. **D77** (2008) 014037, arXiv:0707.2523.

[38] H1 collaboration, A. Aktas *et al.*, *Elastic $J/\psi$ production at HERA*, Eur. Phys. J. **C46** (2006) 585, arXiv:hep-ex/0510016.

[39] ZEUS collaboration, S. Chekanov *et al.*, *Exclusive photoproduction of $J/\psi$ mesons at HERA*, Eur. Phys. J. **C24** (2002) 345, arXiv:hep-ex/0201043.

[40] E. Iancu, K. Itakura, and S. Munier, *Saturation and BFKL dynamics in the HERA data at small $x$*, Phys. Lett. **B590** (2004) 199, arXiv:hep-ph/0310338.

[41] J. Cepila, J. G. Contreras, and M. Krelina, *Coherent and incoherent $J/\psi$ photonuclear production in an energy-dependent hot-spot model*, Phys. Rev. **C97** (2018) 024901, arXiv:1711.01855.

[42] H. Mäntysaari and B. Schenke, *Probing subnucleon scale fluctuations in ultraperipheral heavy ion collisions*, Phys. Lett. **B772** (2017) 832, arXiv:1703.09256.

[43] L. Frankfurt, V. Guzey, and M. Strikman, *Leading twist nuclear shadowing phenomena in hard processes with nuclei*, Phys. Rept. **512** (2012) 255, arXiv:1106.2091.

# LHCb collaboration

R. Aaij[32], C. Abellán Beteta[50], T. Ackernley[60], B. Adeva[46], M. Adinolfi[54], H. Afsharnia[9], C.A. Aidala[86], S. Aiola[25], Z. Ajaltouni[9], S. Akar[65], J. Albrecht[15], F. Alessio[48], M. Alexander[59], A. Alfonso Albero[45], Z. Aliouche[62], G. Alkhazov[38], P. Alvarez Cartelle[55], S. Amato[2], Y. Amhis[11], L. An[48], L. Anderlini[22], A. Andreianov[38], M. Andreotti[21], F. Archilli[17], A. Artamonov[44], M. Artuso[68], K. Arzymatov[42], E. Aslanides[10], M. Atzeni[50], B. Audurier[12], S. Bachmann[17], M. Bachmayer[49], J.J. Back[56], P. Baladron Rodriguez[46], V. Balagura[12], W. Baldini[21], J. Baptista Leite[1], R.J. Barlow[62], S. Barsuk[11], W. Barter[61], M. Bartolini[24], F. Baryshnikov[83], J.M. Basels[14], G. Bassi[29], B. Batsukh[68], A. Battig[15], A. Bay[49], M. Becker[15], F. Bedeschi[29], I. Bediaga[1], A. Beiter[68], V. Belavin[42], S. Belin[27], V. Bellee[49], K. Belous[44], I. Belov[40], I. Belyaev[41], G. Bencivenni[23], E. Ben-Haim[13], A. Berezhnoy[40], R. Bernet[50], D. Berninghoff[17], H.C. Bernstein[68], C. Bertella[48], A. Bertolin[28], C. Betancourt[50], F. Betti[48], Ia. Bezshyiko[50], S. Bhasin[54], J. Bhom[35], L. Bian[73], M.S. Bieker[15], S. Bifani[53], P. Billoir[13], M. Birch[61], F.C.R. Bishop[55], A. Bitadze[62], A. Bizzeti[22,k], M. Bjørn[63], M.P. Blago[48], T. Blake[56], F. Blanc[49], S. Blusk[68], D. Bobulska[59], J.A. Boelhauve[15], O. Boente Garcia[46], T. Boettcher[65], A. Boldyrev[82], A. Bondar[43], N. Bondar[38,48], S. Borghi[62], M. Borisyak[42], M. Borsato[17], J.T. Borsuk[35], S.A. Bouchiba[49], T.J.V. Bowcock[60], A. Boyer[48], C. Bozzi[21], M.J. Bradley[61], S. Braun[66], A. Brea Rodriguez[46], M. Brodski[48], J. Brodzicka[35], A. Brossa Gonzalo[56], D. Brundu[27], A. Buonaura[50], C. Burr[48], A. Bursche[72], A. Butkevich[39], J.S. Butter[32], J. Buytaert[48], W. Byczynski[48], S. Cadeddu[27], H. Cai[73], R. Calabrese[21,f], L. Calefice[15,13], L. Calero Diaz[23], S. Cali[23], R. Calladine[53], M. Calvi[26,j], M. Calvo Gomez[85], P. Camargo Magalhaes[54], A. Camboni[45,85], P. Campana[23], A.F. Campoverde Quezada[6], S. Capelli[26,j], L. Capriotti[20,d], A. Carbone[20,d], G. Carboni[31], R. Cardinale[24], A. Cardini[27], I. Carli[4], P. Carniti[26,j], L. Carus[14], K. Carvalho Akiba[32], A. Casais Vidal[46], G. Casse[60], M. Cattaneo[48], G. Cavallero[48], S. Celani[49], J. Cerasoli[10], A.J. Chadwick[60], M.G. Chapman[54], M. Charles[13], Ph. Charpentier[48], G. Chatzikonstantinidis[53], C.A. Chavez Barajas[60], M. Chefdeville[8], C. Chen[3], S. Chen[4], A. Chernov[35], V. Chobanova[46], S. Cholak[49], M. Chrzaszcz[35], A. Chubykin[38], V. Chulikov[38], P. Ciambrone[23], M.F. Cicala[56], X. Cid Vidal[46], G. Ciezarek[48], P.E.L. Clarke[58], M. Clemencic[48], H.V. Cliff[55], J. Closier[48], J.L. Cobbledick[62], V. Coco[48], J.A.B. Coelho[11], J. Cogan[10], E. Cogneras[9], L. Cojocariu[37], P. Collins[48], T. Colombo[48], L. Congedo[19,c], A. Contu[27], N. Cooke[53], G. Coombs[59], G. Corti[48], C.M. Costa Sobral[56], B. Couturier[48], D.C. Craik[64], J. Crkovská[67], M. Cruz Torres[1], R. Currie[58], C.L. Da Silva[67], E. Dall'Occo[15], J. Dalseno[46], C. D'Ambrosio[48], A. Danilina[41], P. d'Argent[48], A. Davis[62], O. De Aguiar Francisco[62], K. De Bruyn[79], S. De Capua[62], M. De Cian[49], J.M. De Miranda[1], L. De Paula[2], M. De Serio[19,c], D. De Simone[50], P. De Simone[23], J.A. de Vries[80], C.T. Dean[67], D. Decamp[8], L. Del Buono[13], B. Delaney[55], H.-P. Dembinski[15], A. Dendek[34], V. Denysenko[50], D. Derkach[82], O. Deschamps[9], F. Desse[11], F. Dettori[27,e], B. Dey[77], P. Di Nezza[23], S. Didenko[83], L. Dieste Maronas[46], H. Dijkstra[48], V. Dobishuk[52], A.M. Donohoe[18], F. Dordei[27], A.C. dos Reis[1], L. Douglas[59], A. Dovbnya[51], A.G. Downes[8], K. Dreimanis[60], M.W. Dudek[35], L. Dufour[48], V. Duk[78], P. Durante[48], J.M. Durham[67], D. Dutta[62], A. Dziurda[35], A. Dzyuba[38], S. Easo[57], U. Egede[69], V. Egorychev[41], S. Eidelman[43,v], S. Eisenhardt[58], S. Ek-In[49], L. Eklund[59,w], S. Ely[68], A. Ene[37], E. Epple[67], S. Escher[14], J. Eschle[50], S. Esen[13], T. Evans[48], A. Falabella[20], J. Fan[3], Y. Fan[6], B. Fang[73], S. Farry[60], D. Fazzini[26,j], M. Féo[48], A. Fernandez Prieto[46], J.M. Fernandez-tenllado Arribas[45], A.D. Fernez[66], F. Ferrari[20,d], L. Ferreira Lopes[49], F. Ferreira Rodrigues[2], S. Ferreres Sole[32], M. Ferrillo[50], M. Ferro-Luzzi[48], S. Filippov[39], R.A. Fini[19], M. Fiorini[21,f], M. Firlej[34], K.M. Fischer[63], D.S. Fitzgerald[86], C. Fitzpatrick[62], T. Fiutowski[34], F. Fleuret[12], M. Fontana[13], F. Fontanelli[24,h], R. Forty[48], V. Franco Lima[60], M. Franco Sevilla[66], M. Frank[48], E. Franzoso[21], G. Frau[17], C. Frei[48], D.A. Friday[59], J. Fu[25], Q. Fuehring[15], W. Funk[48], E. Gabriel[32],

T. Gaintseva[42], A. Gallas Torreira[46], D. Galli[20,d], S. Gambetta[58,48], Y. Gan[3], M. Gandelman[2], P. Gandini[25], Y. Gao[5], M. Garau[27], L.M. Garcia Martin[56], P. Garcia Moreno[45], J. García Pardiñas[26,j], B. Garcia Plana[46], F.A. Garcia Rosales[12], L. Garrido[45], C. Gaspar[48], R.E. Geertsema[32], D. Gerick[17], L.L. Gerken[15], E. Gersabeck[62], M. Gersabeck[62], T. Gershon[56], D. Gerstel[10], Ph. Ghez[8], V. Gibson[55], H.K. Giemza[36], M. Giovannetti[23,p], A. Gioventù[46], P. Gironella Gironell[45], L. Giubega[37], C. Giugliano[21,f,48], K. Gizdov[58], E.L. Gkougkousis[48], V.V. Gligorov[13], C. Göbel[70], E. Golobardes[85], D. Golubkov[41], A. Golutvin[61,83], A. Gomes[1,a], S. Gomez Fernandez[45], F. Goncalves Abrantes[63], M. Goncerz[35], G. Gong[3], P. Gorbounov[41], I.V. Gorelov[40], C. Gotti[26], E. Govorkova[48], J.P. Grabowski[17], T. Grammatico[13], L.A. Granado Cardoso[48], E. Graugés[45], E. Graverini[49], G. Graziani[22], A. Grecu[37], L.M. Greeven[32], P. Griffith[21,f], L. Grillo[62], S. Gromov[83], B.R. Gruberg Cazon[63], C. Gu[3], M. Guarise[21], P. A. Günther[17], E. Gushchin[39], A. Guth[14], Y. Guz[44], T. Gys[48], T. Hadavizadeh[69], G. Haefeli[49], C. Haen[48], J. Haimberger[48], T. Halewood-leagas[60], P.M. Hamilton[66], J.P. Hammerich[60], Q. Han[7], X. Han[17], T.H. Hancock[63], S. Hansmann-Menzemer[17], N. Harnew[63], T. Harrison[60], C. Hasse[48], M. Hatch[48], J. He[6,b], M. Hecker[61], K. Heijhoff[32], K. Heinicke[15], A.M. Hennequin[48], K. Hennessy[60], L. Henry[25,47], J. Heuel[14], A. Hicheur[2], D. Hill[49], M. Hilton[62], S.E. Hollitt[15], J. Hu[17], J. Hu[72], W. Hu[7], W. Huang[6], X. Huang[73], W. Hulsbergen[32], R.J. Hunter[56], M. Hushchyn[82], D. Hutchcroft[60], D. Hynds[32], P. Ibis[15], M. Idzik[34], D. Ilin[38], P. Ilten[65], A. Inglessi[38], A. Ishteev[83], K. Ivshin[38], R. Jacobsson[48], S. Jakobsen[48], E. Jans[32], B.K. Jashal[47], A. Jawahery[66], V. Jevtic[15], M. Jezabek[35], F. Jiang[3], M. John[63], D. Johnson[48], C.R. Jones[55], T.P. Jones[56], B. Jost[48], N. Jurik[48], S. Kandybei[51], Y. Kang[3], M. Karacson[48], M. Karpov[82], F. Keizer[48], M. Kenzie[56], T. Ketel[33], B. Khanji[15], A. Kharisova[84], S. Kholodenko[44], T. Kirn[14], V.S. Kirsebom[49], O. Kitouni[64], S. Klaver[32], K. Klimaszewski[36], S. Koliiev[52], A. Kondybayeva[83], A. Konoplyannikov[41], P. Kopciewicz[34], R. Kopecna[17], P. Koppenburg[32], M. Korolev[40], I. Kostiuk[32,52], O. Kot[52], S. Kotriakhova[21,38], P. Kravchenko[38], L. Kravchuk[39], R.D. Krawczyk[48], M. Kreps[56], F. Kress[61], S. Kretzschmar[14], P. Krokovny[43,v], W. Krupa[34], W. Krzemien[36], W. Kucewicz[35,t], M. Kucharczyk[35], V. Kudryavtsev[43,v], H.S. Kuindersma[32,33], G.J. Kunde[67], T. Kvaratskheliya[41], D. Lacarrere[48], G. Lafferty[62], A. Lai[27], A. Lampis[27], D. Lancierini[50], J.J. Lane[62], R. Lane[54], G. Lanfranchi[23], C. Langenbruch[14], J. Langer[15], O. Lantwin[50], T. Latham[56], F. Lazzari[29,q], R. Le Gac[10], S.H. Lee[86], R. Lefèvre[9], A. Leflat[40], S. Legotin[83], O. Leroy[10], T. Lesiak[35], B. Leverington[17], H. Li[72], L. Li[63], P. Li[17], S. Li[7], Y. Li[4], Y. Li[4], Z. Li[68], X. Liang[68], T. Lin[61], R. Lindner[48], V. Lisovskyi[15], R. Litvinov[27], G. Liu[72], H. Liu[6], S. Liu[4], X. Liu[3], A. Loi[27], J. Lomba Castro[46], I. Longstaff[59], J.H. Lopes[2], G.H. Lovell[55], Q. Lu[72], Y. Lu[4], D. Lucchesi[28,l], S. Luchuk[39], M. Lucio Martinez[32], V. Lukashenko[32,52], Y. Luo[3], A. Lupato[62], E. Luppi[21,f], O. Lupton[56], A. Lusiani[29,m], X. Lyu[6], L. Ma[4], R. Ma[6], S. Maccolini[20,d], F. Machefert[11], F. Maciuc[37], V. Macko[49], P. Mackowiak[15], S. Maddrell-Mander[54], O. Madejczyk[34], L.R. Madhan Mohan[54], O. Maev[38], A. Maevskiy[82], D. Maisuzenko[38], M.W. Majewski[34], J.J. Malczewski[35], S. Malde[63], B. Malecki[48], A. Malinin[81], T. Maltsev[43,v], H. Malygina[17], G. Manca[27,e], G. Mancinelli[10], D. Manuzzi[20,d], D. Marangotto[25,i], J. Maratas[9,s], J.F. Marchand[8], U. Marconi[20], S. Mariani[22,g], C. Marin Benito[48], M. Marinangeli[49], J. Marks[17], A.M. Marshall[54], P.J. Marshall[60], G. Martellotti[30], L. Martinazzoli[48,j], M. Martinelli[26,j], D. Martinez Santos[46], F. Martinez Vidal[47], A. Massafferri[1], M. Materok[14], R. Matev[48], A. Mathad[50], Z. Mathe[48], V. Matiunin[41], C. Matteuzzi[26], K.R. Mattioli[86], A. Mauri[32], E. Maurice[12], J. Mauricio[45], M. Mazurek[48], M. McCann[61], L. Mcconnell[18], T.H. Mcgrath[62], A. McNab[62], R. McNulty[18], J.V. Mead[60], B. Meadows[65], C. Meaux[10], G. Meier[15], N. Meinert[76], D. Melnychuk[36], S. Meloni[26,j], M. Merk[32,80], A. Merli[25], L. Meyer Garcia[2], M. Mikhasenko[48], D.A. Milanes[74], E. Millard[56], M. Milovanovic[48], M.-N. Minard[8], A. Minotti[21], L. Minzoni[21,f], S.E. Mitchell[58], B. Mitreska[62], D.S. Mitzel[48], A. Mödden [15], R.A. Mohammed[63], R.D. Moise[61], T. Mombächer[15],

I.A. Monroy[74], S. Monteil[9], M. Morandin[28], G. Morello[23], M.J. Morello[29,m], J. Moron[34], A.B. Morris[75], A.G. Morris[56], R. Mountain[68], H. Mu[3], F. Muheim[58,48], M. Mulder[48], D. Müller[48], K. Müller[50], C.H. Murphy[63], D. Murray[62], P. Muzzetto[27,48], P. Naik[54], T. Nakada[49], R. Nandakumar[57], T. Nanut[49], I. Nasteva[2], M. Needham[58], I. Neri[21], N. Neri[25,i], S. Neubert[75], N. Neufeld[48], R. Newcombe[61], T.D. Nguyen[49], C. Nguyen-Mau[49,x], E.M. Niel[11], S. Nieswand[14], N. Nikitin[40], N.S. Nolte[15], C. Nunez[86], A. Oblakowska-Mucha[34], V. Obraztsov[44], D.P. O'Hanlon[54], R. Oldeman[27,e], M.E. Olivares[68], C.J.G. Onderwater[79], A. Ossowska[35], J.M. Otalora Goicochea[2], T. Ovsiannikova[41], P. Owen[50], A. Oyanguren[47], B. Pagare[56], P.R. Pais[48], T. Pajero[63], A. Palano[19], M. Palutan[23], Y. Pan[62], G. Panshin[84], A. Papanestis[57], M. Pappagallo[19,c], L.L. Pappalardo[21,f], C. Pappenheimer[65], W. Parker[66], C. Parkes[62], C.J. Parkinson[46], B. Passalacqua[21], G. Passaleva[22], A. Pastore[19], M. Patel[61], C. Patrignani[20,d], C.J. Pawley[80], A. Pearce[48], A. Pellegrino[32], M. Pepe Altarelli[48], S. Perazzini[20], D. Pereima[41], P. Perret[9], M. Petric[59,48], K. Petridis[54], A. Petrolini[24,h], A. Petrov[81], S. Petrucci[58], M. Petruzzo[25], T.T.H. Pham[68], A. Philippov[42], L. Pica[29,m], M. Piccini[78], B. Pietrzyk[8], G. Pietrzyk[49], M. Pili[63], D. Pinci[30], F. Pisani[48], Resmi P.K[10], V. Placinta[37], J. Plews[53], M. Plo Casasus[46], F. Polci[13], M. Poli Lener[23], M. Poliakova[68], A. Poluektov[10], N. Polukhina[83,u], I. Polyakov[68], E. Polycarpo[2], G.J. Pomery[54], S. Ponce[48], D. Popov[6,48], S. Popov[42], S. Poslavskii[44], K. Prasanth[35], L. Promberger[48], C. Prouve[46], V. Pugatch[52], H. Pullen[63], G. Punzi[29,n], W. Qian[6], J. Qin[6], R. Quagliani[13], B. Quintana[8], N.V. Raab[18], R.I. Rabadan Trejo[10], B. Rachwal[34], J.H. Rademacker[54], M. Rama[29], M. Ramos Pernas[56], M.S. Rangel[2], F. Ratnikov[42,82], G. Raven[33], M. Reboud[8], F. Redi[49], F. Reiss[62], C. Remon Alepuz[47], Z. Ren[3], V. Renaudin[63], R. Ribatti[29], S. Ricciardi[57], K. Rinnert[60], P. Robbe[11], G. Robertson[58], A.B. Rodrigues[49], E. Rodrigues[60], J.A. Rodriguez Lopez[74], A. Rollings[63], P. Roloff[48], V. Romanovskiy[44], M. Romero Lamas[46], A. Romero Vidal[46], J.D. Roth[86], M. Rotondo[23], M.S. Rudolph[68], T. Ruf[48], J. Ruiz Vidal[47], A. Ryzhikov[82], J. Ryzka[34], J.J. Saborido Silva[46], N. Sagidova[38], N. Sahoo[56], B. Saitta[27,e], M. Salomoni[48], D. Sanchez Gonzalo[45], C. Sanchez Gras[32], R. Santacesaria[30], C. Santamarina Rios[46], M. Santimaria[23], E. Santovetti[31,p], D. Saranin[83], G. Sarpis[62], M. Sarpis[75], A. Sarti[30], C. Satriano[30,o], A. Satta[31], M. Saur[15], D. Savrina[41,40], H. Sazak[9], L.G. Scantlebury Smead[63], S. Schael[14], M. Schellenberg[15], M. Schiller[59], H. Schindler[48], M. Schmelling[16], B. Schmidt[48], O. Schneider[49], A. Schopper[48], M. Schubiger[32], S. Schulte[49], M.H. Schune[11], R. Schwemmer[48], B. Sciascia[23], S. Sellam[46], A. Semennikov[41], M. Senghi Soares[33], A. Sergi[24], N. Serra[50], L. Sestini[28], A. Seuthe[15], P. Seyfert[48], Y. Shang[5], D.M. Shangase[86], M. Shapkin[44], I. Shchemerov[83], L. Shchutska[49], T. Shears[60], L. Shekhtman[43,v], Z. Shen[5], V. Shevchenko[81], E.B. Shields[26,j], E. Shmanin[83], J.D. Shupperd[68], B.G. Siddi[21], R. Silva Coutinho[50], G. Simi[28], S. Simone[19,c], N. Skidmore[62], T. Skwarnicki[68], M.W. Slater[53], I. Slazyk[21,f], J.C. Smallwood[63], J.G. Smeaton[55], A. Smetkina[41], E. Smith[50], M. Smith[61], A. Snoch[32], M. Soares[20], L. Soares Lavra[9], M.D. Sokoloff[65], F.J.P. Soler[59], A. Solovev[38], I. Solovyev[38], F.L. Souza De Almeida[2], B. Souza De Paula[2], B. Spaan[15], E. Spadaro Norella[25,i], P. Spradlin[59], F. Stagni[48], M. Stahl[65], S. Stahl[48], P. Stefko[49], O. Steinkamp[50,83], O. Stenyakin[44], H. Stevens[15], S. Stone[68], M.E. Stramaglia[49], M. Straticiuc[37], D. Strekalina[83], F. Suljik[63], J. Sun[27], L. Sun[73], Y. Sun[66], P. Svihra[62], P.N. Swallow[53], K. Swientek[34], A. Szabelski[36], T. Szumlak[34], M. Szymanski[48], S. Taneja[62], F. Teubert[48], E. Thomas[48], K.A. Thomson[60], V. Tisserand[9], S. T'Jampens[8], M. Tobin[4], L. Tomassetti[21,f], D. Torres Machado[1], D.Y. Tou[13], M.T. Tran[49], E. Trifonova[83], C. Trippl[49], G. Tuci[29,n], A. Tully[49], N. Tuning[32,48], A. Ukleja[36], D.J. Unverzagt[17], E. Ursov[83], A. Usachov[32], A. Ustyuzhanin[42,82], U. Uwer[17], A. Vagner[84], V. Vagnoni[20], A. Valassi[48], G. Valenti[20], N. Valls Canudas[85], M. van Beuzekom[32], M. Van Dijk[49], E. van Herwijnen[83], C.B. Van Hulse[18], M. van Veghel[79], R. Vazquez Gomez[46], P. Vazquez Regueiro[46], C. Vázquez Sierra[48], S. Vecchi[21], J.J. Velthuis[54], M. Veltri[22,r], A. Venkateswaran[68], M. Veronesi[32], M. Vesterinen[56], D. Vieira[65], M. Vieites Diaz[49],

H. Viemann[76], X. Vilasis-Cardona[85], E. Vilella Figueras[60], P. Vincent[13], D. Vom Bruch[10], A. Vorobyev[38], V. Vorobyev[43,v], N. Voropaev[38], R. Waldi[17], J. Walsh[29], C. Wang[17], J. Wang[5], J. Wang[4], J. Wang[3], J. Wang[73], M. Wang[3], R. Wang[54], Y. Wang[7], Z. Wang[50], Z. Wang[3], H.M. Wark[60], N.K. Watson[53], S.G. Weber[13], D. Websdale[61], C. Weisser[64], B.D.C. Westhenry[54], D.J. White[62], M. Whitehead[54], D. Wiedner[15], G. Wilkinson[63], M. Wilkinson[68], I. Williams[55], M. Williams[64], M.R.J. Williams[58], F.F. Wilson[57], W. Wislicki[36], M. Witek[35], L. Witola[17], G. Wormser[11], S.A. Wotton[55], H. Wu[68], K. Wyllie[48], Z. Xiang[6], D. Xiao[7], Y. Xie[7], A. Xu[5], J. Xu[6], L. Xu[3], M. Xu[7], Q. Xu[6], Z. Xu[5], Z. Xu[6], D. Yang[3], S. Yang[6], Y. Yang[6], Z. Yang[3], Z. Yang[66], Y. Yao[68], L.E. Yeomans[60], H. Yin[7], J. Yu[71], X. Yuan[68], O. Yushchenko[44], E. Zaffaroni[49], M. Zavertyaev[16,u], M. Zdybal[35], O. Zenaiev[48], M. Zeng[3], D. Zhang[7], L. Zhang[3], S. Zhang[5], Y. Zhang[5], Y. Zhang[63], A. Zhelezov[17], Y. Zheng[6], X. Zhou[6], Y. Zhou[6], X. Zhu[3], Z. Zhu[6], V. Zhukov[14,40], J.B. Zonneveld[58], Q. Zou[4], S. Zucchelli[20,d], D. Zuliani[28], G. Zunica[62].

[1] *Centro Brasileiro de Pesquisas Físicas (CBPF), Rio de Janeiro, Brazil*
[2] *Universidade Federal do Rio de Janeiro (UFRJ), Rio de Janeiro, Brazil*
[3] *Center for High Energy Physics, Tsinghua University, Beijing, China*
[4] *Institute Of High Energy Physics (IHEP), Beijing, China*
[5] *School of Physics State Key Laboratory of Nuclear Physics and Technology, Peking University, Beijing, China*
[6] *University of Chinese Academy of Sciences, Beijing, China*
[7] *Institute of Particle Physics, Central China Normal University, Wuhan, Hubei, China*
[8] *Univ. Savoie Mont Blanc, CNRS, IN2P3-LAPP, Annecy, France*
[9] *Université Clermont Auvergne, CNRS/IN2P3, LPC, Clermont-Ferrand, France*
[10] *Aix Marseille Univ, CNRS/IN2P3, CPPM, Marseille, France*
[11] *Université Paris-Saclay, CNRS/IN2P3, IJCLab, Orsay, France*
[12] *Laboratoire Leprince-Ringuet, CNRS/IN2P3, Ecole Polytechnique, Institut Polytechnique de Paris, Palaiseau, France*
[13] *LPNHE, Sorbonne Université, Paris Diderot Sorbonne Paris Cité, CNRS/IN2P3, Paris, France*
[14] *I. Physikalisches Institut, RWTH Aachen University, Aachen, Germany*
[15] *Fakultät Physik, Technische Universität Dortmund, Dortmund, Germany*
[16] *Max-Planck-Institut für Kernphysik (MPIK), Heidelberg, Germany*
[17] *Physikalisches Institut, Ruprecht-Karls-Universität Heidelberg, Heidelberg, Germany*
[18] *School of Physics, University College Dublin, Dublin, Ireland*
[19] *INFN Sezione di Bari, Bari, Italy*
[20] *INFN Sezione di Bologna, Bologna, Italy*
[21] *INFN Sezione di Ferrara, Ferrara, Italy*
[22] *INFN Sezione di Firenze, Firenze, Italy*
[23] *INFN Laboratori Nazionali di Frascati, Frascati, Italy*
[24] *INFN Sezione di Genova, Genova, Italy*
[25] *INFN Sezione di Milano, Milano, Italy*
[26] *INFN Sezione di Milano-Bicocca, Milano, Italy*
[27] *INFN Sezione di Cagliari, Monserrato, Italy*
[28] *Universita degli Studi di Padova, Universita e INFN, Padova, Padova, Italy*
[29] *INFN Sezione di Pisa, Pisa, Italy*
[30] *INFN Sezione di Roma La Sapienza, Roma, Italy*
[31] *INFN Sezione di Roma Tor Vergata, Roma, Italy*
[32] *Nikhef National Institute for Subatomic Physics, Amsterdam, Netherlands*
[33] *Nikhef National Institute for Subatomic Physics and VU University Amsterdam, Amsterdam, Netherlands*
[34] *AGH - University of Science and Technology, Faculty of Physics and Applied Computer Science, Kraków, Poland*
[35] *Henryk Niewodniczanski Institute of Nuclear Physics Polish Academy of Sciences, Kraków, Poland*
[36] *National Center for Nuclear Research (NCBJ), Warsaw, Poland*
[37] *Horia Hulubei National Institute of Physics and Nuclear Engineering, Bucharest-Magurele, Romania*
[38] *Petersburg Nuclear Physics Institute NRC Kurchatov Institute (PNPI NRC KI), Gatchina, Russia*

[39] *Institute for Nuclear Research of the Russian Academy of Sciences (INR RAS), Moscow, Russia*
[40] *Institute of Nuclear Physics, Moscow State University (SINP MSU), Moscow, Russia*
[41] *Institute of Theoretical and Experimental Physics NRC Kurchatov Institute (ITEP NRC KI), Moscow, Russia*
[42] *Yandex School of Data Analysis, Moscow, Russia*
[43] *Budker Institute of Nuclear Physics (SB RAS), Novosibirsk, Russia*
[44] *Institute for High Energy Physics NRC Kurchatov Institute (IHEP NRC KI), Protvino, Russia, Protvino, Russia*
[45] *ICCUB, Universitat de Barcelona, Barcelona, Spain*
[46] *Instituto Galego de Física de Altas Enerxías (IGFAE), Universidade de Santiago de Compostela, Santiago de Compostela, Spain*
[47] *Instituto de Fisica Corpuscular, Centro Mixto Universidad de Valencia - CSIC, Valencia, Spain*
[48] *European Organization for Nuclear Research (CERN), Geneva, Switzerland*
[49] *Institute of Physics, Ecole Polytechnique Fédérale de Lausanne (EPFL), Lausanne, Switzerland*
[50] *Physik-Institut, Universität Zürich, Zürich, Switzerland*
[51] *NSC Kharkiv Institute of Physics and Technology (NSC KIPT), Kharkiv, Ukraine*
[52] *Institute for Nuclear Research of the National Academy of Sciences (KINR), Kyiv, Ukraine*
[53] *University of Birmingham, Birmingham, United Kingdom*
[54] *H.H. Wills Physics Laboratory, University of Bristol, Bristol, United Kingdom*
[55] *Cavendish Laboratory, University of Cambridge, Cambridge, United Kingdom*
[56] *Department of Physics, University of Warwick, Coventry, United Kingdom*
[57] *STFC Rutherford Appleton Laboratory, Didcot, United Kingdom*
[58] *School of Physics and Astronomy, University of Edinburgh, Edinburgh, United Kingdom*
[59] *School of Physics and Astronomy, University of Glasgow, Glasgow, United Kingdom*
[60] *Oliver Lodge Laboratory, University of Liverpool, Liverpool, United Kingdom*
[61] *Imperial College London, London, United Kingdom*
[62] *Department of Physics and Astronomy, University of Manchester, Manchester, United Kingdom*
[63] *Department of Physics, University of Oxford, Oxford, United Kingdom*
[64] *Massachusetts Institute of Technology, Cambridge, MA, United States*
[65] *University of Cincinnati, Cincinnati, OH, United States*
[66] *University of Maryland, College Park, MD, United States*
[67] *Los Alamos National Laboratory (LANL), Los Alamos, United States*
[68] *Syracuse University, Syracuse, NY, United States*
[69] *School of Physics and Astronomy, Monash University, Melbourne, Australia, associated to* [56]
[70] *Pontifícia Universidade Católica do Rio de Janeiro (PUC-Rio), Rio de Janeiro, Brazil, associated to* [2]
[71] *Physics and Micro Electronic College, Hunan University, Changsha City, China, associated to* [7]
[72] *Guangdong Provincial Key Laboratory of Nuclear Science, Guangdong-Hong Kong Joint Laboratory of Quantum Matter, Institute of Quantum Matter, South China Normal University, Guangzhou, China, associated to* [3]
[73] *School of Physics and Technology, Wuhan University, Wuhan, China, associated to* [3]
[74] *Departamento de Fisica , Universidad Nacional de Colombia, Bogota, Colombia, associated to* [13]
[75] *Universität Bonn - Helmholtz-Institut für Strahlen und Kernphysik, Bonn, Germany, associated to* [17]
[76] *Institut für Physik, Universität Rostock, Rostock, Germany, associated to* [17]
[77] *Eotvos Lorand University, Budapest, Hungary, associated to* [48]
[78] *INFN Sezione di Perugia, Perugia, Italy, associated to* [21]
[79] *Van Swinderen Institute, University of Groningen, Groningen, Netherlands, associated to* [32]
[80] *Universiteit Maastricht, Maastricht, Netherlands, associated to* [32]
[81] *National Research Centre Kurchatov Institute, Moscow, Russia, associated to* [41]
[82] *National Research University Higher School of Economics, Moscow, Russia, associated to* [42]
[83] *National University of Science and Technology "MISIS", Moscow, Russia, associated to* [41]
[84] *National Research Tomsk Polytechnic University, Tomsk, Russia, associated to* [41]
[85] *DS4DS, La Salle, Universitat Ramon Llull, Barcelona, Spain, associated to* [45]
[86] *University of Michigan, Ann Arbor, United States, associated to* [68]

[a] *Universidade Federal do Triângulo Mineiro (UFTM), Uberaba-MG, Brazil*
[b] *Hangzhou Institute for Advanced Study, UCAS, Hangzhou, China*
[c] *Università di Bari, Bari, Italy*

[d] *Università di Bologna, Bologna, Italy*
[e] *Università di Cagliari, Cagliari, Italy*
[f] *Università di Ferrara, Ferrara, Italy*
[g] *Università di Firenze, Firenze, Italy*
[h] *Università di Genova, Genova, Italy*
[i] *Università degli Studi di Milano, Milano, Italy*
[j] *Università di Milano Bicocca, Milano, Italy*
[k] *Università di Modena e Reggio Emilia, Modena, Italy*
[l] *Università di Padova, Padova, Italy*
[m] *Scuola Normale Superiore, Pisa, Italy*
[n] *Università di Pisa, Pisa, Italy*
[o] *Università della Basilicata, Potenza, Italy*
[p] *Università di Roma Tor Vergata, Roma, Italy*
[q] *Università di Siena, Siena, Italy*
[r] *Università di Urbino, Urbino, Italy*
[s] *MSU - Iligan Institute of Technology (MSU-IIT), Iligan, Philippines*
[t] *AGH - University of Science and Technology, Faculty of Computer Science, Electronics and Telecommunications, Kraków, Poland*
[u] *P.N. Lebedev Physical Institute, Russian Academy of Science (LPI RAS), Moscow, Russia*
[v] *Novosibirsk State University, Novosibirsk, Russia*
[w] *Department of Physics and Astronomy, Uppsala University, Uppsala, Sweden*
[x] *Hanoi University of Science, Hanoi, Vietnam*